

# A Fast Ray-Tracing Method for Microstrip Rotman Lens Analysis

*Junwei Dong<sup>1</sup>, Amir I. Zaghloul<sup>1</sup>, Ruth Rotman<sup>2</sup>*

<sup>1</sup> Virginia Polytechnic Institute and State University, VA 22043, USA  
[djwei@vt.edu](mailto:djwei@vt.edu), [amirz@vt.edu](mailto:amirz@vt.edu)

<sup>2</sup> IAI Elta Electronics Industries, Ashdod, Israel  
[rotman@eng.tau.ac.il](mailto:rotman@eng.tau.ac.il)

## Abstract

The optimization of microstrip Rotman lens prior to its fabrication involves considerable iterations and integration between the structure and its performance. The existing full wave solvers can be computationally expensive for simulating such electrically large structure. Driven by the initial need for a fast simulation method for the Rotman lens structure, we propose a ray tracing method to handle the couplings and multi-reflections within the lens cavity. In this paper, the ray tracing design scheme is described and results are shown and compared with the CST/Microwave Studio full wave analysis results.

## 1. Introduction

Since the first Rotman Lens was proposed in 1960s [1], it has been adopted extensively in communication systems as a beam forming vehicle. The nowadays printed circuit technology allows for accurate and inexpensive fabrication of the microstrip Rotman lens. In the lens design, one follows the conventional equations of multiple-focal-point design [1-3] or optimized non-focal lens design method [4] to locate the beam and inner receiving port phase centers. This is followed by choosing proper taper to represent the printed port. There are variety of parameters to determine the ultimate structure of the lens, which eventually determine the qualities of the amplitude and phase coupling between the beam and receiving ports. To evaluate the port-to-port coupling performance of different Rotman lens structures, researchers have attempted the asymptotic equations [5] and full wave analysis [6]. The former is a fast calculation but does not account for the multiple reflections within the lens cavity, hence lacking accuracy. The latter is well known for its accuracy; however the computation is time consuming, hence lacking computational efficiency. A simulation method that is fast and appropriately accurate is still desirable in the Rotman lens design.

The ray tracing method has been largely adopted in designs of large antennas such as reflectors. Its fundamental ray model affects the theory's liability and the number of rays usually guarantees its accuracy. To our knowledge, the full ray tracing method has not been fully applied to simulate a large microstrip structure such as Rotman lens. In this paper, we propose a ray tracing model for the Rotman lens design environment where the multi-reflections inside the lens and their interactions with the taper models are accounted for. A test example is shown via simulating a C-band microstrip lens, and its results are compared with the ones achieved by CST/Microwave Studio full wave analysis.

## 2. Ray Tracing Model for Rotman Lens Design

Figure 1 shows a general Rotman lens structure, without the transmission lines connected to the tapered ends on both sides of the lens. To estimate the coupling between any two ports, e.g. A and D, we need to consider at least three contributors, 1) the reflection coefficient for the beam port taper AB, 2) the direct line of sight coupling between B and C, 3) the reflection coefficient for the receiving port taper CD. The three contributors are combined into a direct coupling factor  $l_i$  between A and D. Besides the direct coupling, there are reflections off other ports that result in signals in the direction of the receiving port, e.g. reflections off ports Z and N represented by coupling factors  $l_i$  and  $l_j$ , respectively. The reradiated or reflected rays couple with all ports causing secondary couplings. The ultimate coupling result between A and D is the sum of the direct coupling and all secondary couplings.

The reflection coefficients that affect the coupling factors are functions of the impedance model at the radiating elements, which is in turn function of the physical taper of the elements. Several types of impedance models can be adopted in the Rotman lens design, such as linear, triangular, exponential, Klopfenstein and Chebyshev tapers. Different models have different reflection patterns versus frequency. Existing approaches of

analyzing the microstrip tapers are: small reflection theory [7], contour integral method [8], and general non-uniform line theory [9]. We use the small reflection theory as our model because of its simplicity. Equations (1) and (2) give the reflection coefficients for the “exponential” and “triangular” impedance models, respectively. It should be mentioned that these models do not necessarily represent the physical taper, e.g. the triangular shape that is shown in Figure 1. The models in equations (1) and (2) are simply defined by their impedance characteristic instead of the shape of the taper. To accurately simulate the model of the physical triangular shape taper that is easy to fabricate, as adopted in many previous design examples [10, 11], we use the polynomial equation to fit the impedance curve as given in equation (3). By using the little reflection theory, the reflection coefficient can be expressed by equation (4).

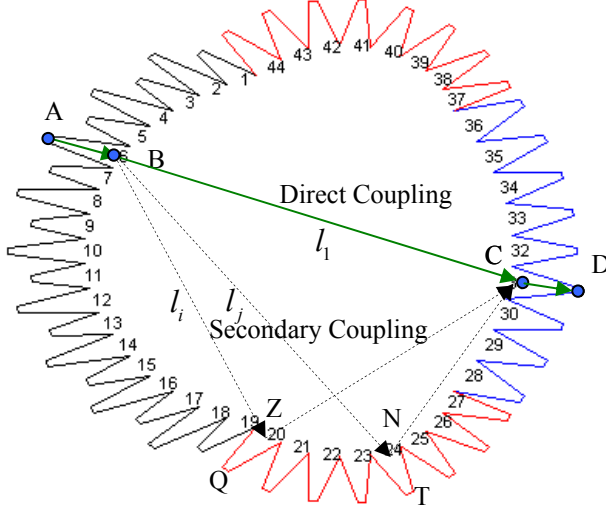


Figure 1. Ray Trace Model for Rotman Lens Design

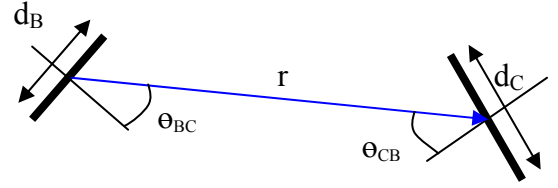


Figure 2. Port to Port Coupling Model

$$\Gamma_{\text{exp}} = \frac{\ln Z_L / Z_0}{2} \frac{\sin(kL)}{kL} e^{-jkL} \quad (1)$$

$$\Gamma_{\text{tri}} = \frac{\ln Z_L / Z_0}{2} \left[ \frac{\sin(kL/2)}{kL/2} \right]^2 e^{-jkL} \quad (2)$$

$$Z(z) = Z_0 \sum_{i=0}^{N=3} a_i z^i \quad (3)$$

$$\Gamma_{\text{pol}} = \frac{1}{2} \int_0^L e^{-2jkz} \frac{d}{dz} \ln \left( \frac{Z(z)}{Z_0} \right) dz = \int_0^L \frac{1}{2} e^{-2jkz} \frac{3a_3 z^2 + 2a_2 z + a_1}{a_3 z^3 + a_2 z^2 + a_1 z + a_0} dz \quad (4)$$

where  $L$  is length of the taper and  $z$  is reference distance to the edge of the taper input.

The port-to-port coupling, discussed above, determines how much energy is coupled between the ports, which is a function of the port sizes, port pointing directions and port-to-port distance, as shown in Figure 2. This model has been studied by using the two dimension aperture theory [12], the mode matching method [13], and the simplified ray equation model [14]. Each of the three models can be used as the port-to-port coupling model in the ray tracing process. The ray tracing analysis in this paper uses the two dimension aperture theory [12], and is represented by equation (5).

$$E_C = E_B * \sqrt{\frac{1}{\lambda r}} d_B \sin c \left( \frac{d_B \sin \theta_{BC}}{\lambda} \right) \cos(\theta_{BC}) \sin c \left( \frac{kd_C}{2} \sin \theta_{CB} \right) \cos(\theta_{CB}) e^{-j(kr - \pi/4)} \quad (5)$$

As mentioned above, the combination of any port-to-port coupling involves direct coupling and secondary couplings. Take ports AB and CD in Figure 1 for example; the final coupling coefficient is expressed in equation (6). The direct coupling shall combine the taper coefficient and the port to port aperture coupling as well, and it is expressed in equation (7). The secondary coupling shall combine all reflections from all other ports, which is expressed in equation (8).

$$E_{DA} = E_{DA(direct)} + E_{DA(indirect)} \quad (6)$$

$$E_{DA(direct)} = E_A * (1 - \Gamma_{AB}) * E_A(\theta_{BC}, d_A) E_D(\theta_{CB}, d_D) (1 + \Gamma_{DC}) * L_{AD} \quad (7)$$

$$E_{DA(indirect)} = \sum_{n=1}^{N=P-1} E_A (1 - \Gamma_{AB}) E_A(\theta_{BZ}, d_A) L_{AQ} * E_Q(\theta_{ZB}, d_Q) (-\Gamma_{QZ}) * E_Q(\theta_{ZC}, d_Q) E_D(\theta_{DZ}, d_D) L_{ZD} * (1 + \Gamma_{DC}) \quad (8)$$

where  $L$  is the path loss factor and  $k$  is the wave number, which is a function of the material dielectric constant, loss tangent and frequency as given in (9).

$$k = k' - jk'' = \omega \sqrt{\mu \epsilon_r} \left(1 - j \frac{\delta}{2}\right) \quad (9)$$

In summary, the ray tracing results between port A and D can be calculated by using equation (6), which combines all other equations and prior information including the materials and structure dimensions. The calculation can be fast due to the closed-form formulas. One test case is demonstrated in the next section.

### 3. Simulation of C-Band Rotman Lens

The lens under test shown in Figure 3 is designed at C-band and has 20 beam ports and 36 receiving ports, with dimensions 280mm X 330mm. The beam port is denoted as 1, receiving port is denoted as 2, and all dummy ports have signs of 0, all marked at the narrow ends of the ports in Figure 3. One test case was done from 3-10 GHz, with excitation port 24, as shown in Figure 3. The amplitude couplings from beam port 24 to all receiving ports simulated by both ray tracing algorithms and CST full wave analysis at 6.5 GHz are shown in Figure 4. The coupling between port 24 to port 70 across the frequency band 3-10GHz is shown in Figure 5 and 6, for amplitude and phase couplings; respectively, similar results between port 24 and port 80 are shown in Figure 7 and 8.

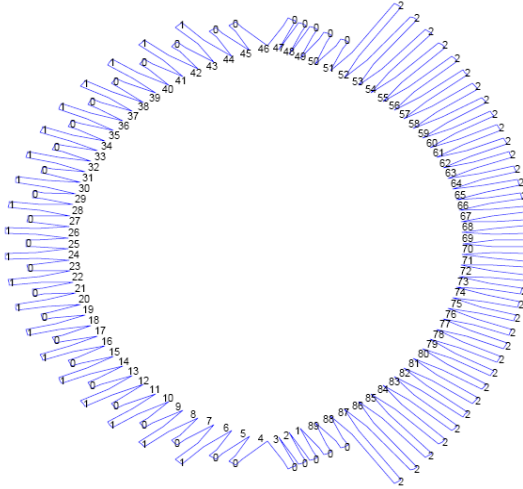


Figure 3. C Band Rotman Lens under Test, 1 stands for beam port, 0 dummy port, and 2 is the receiving port

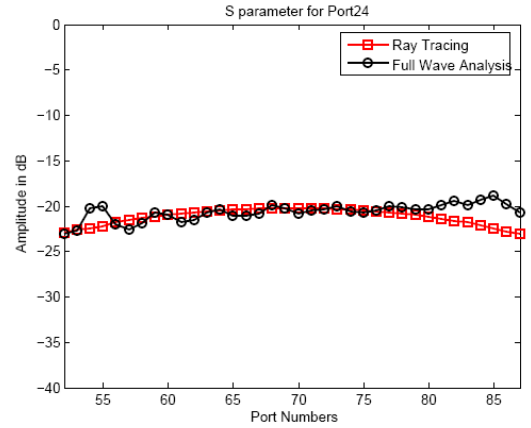


Figure 4. The amplitude coupling between port 24 and all receiving ports 52-87. The experiment was conducted at frequency 6.5 GHz, all port are terminated by 50 ohm

It is noticed that the simulation of ray tracing in this example took about 10 seconds, comparatively, the computation time for CST was approximately 1.5 hours. Comparison of the two results show the match between the amplitude couplings for the two methods is superior to the phase couplings, which may be possibly due to certain phase reference plane shift in either of the simulation programs.

### 4. Conclusion

A ray tracing method of analyzing the Rotman Lens is proposed in this paper. The simulation of a C-band lens using this method was compared with the results of CST full wave analysis. Good agreements were shown, which demonstrated that the ray tracing method is a computationally efficient approach to simulate the electronically large Rotman Lens structure.

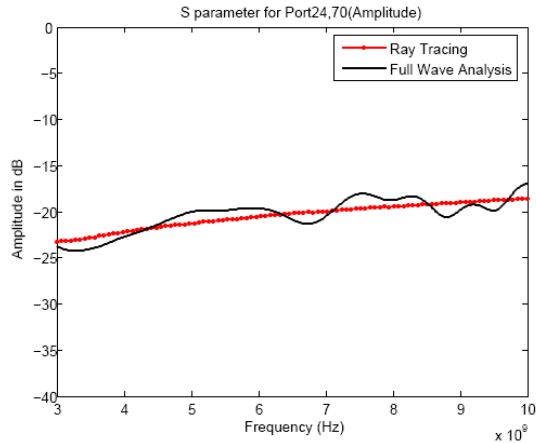


Figure 5. The amplitude coupling between port 24 and receiving port 70 across frequency band 3-10GHz.

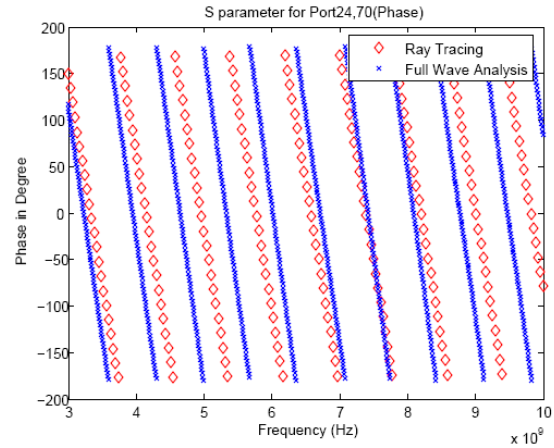


Figure 6. The phase coupling between port 24 and receiving port 70 across frequency band 3-10GHz.

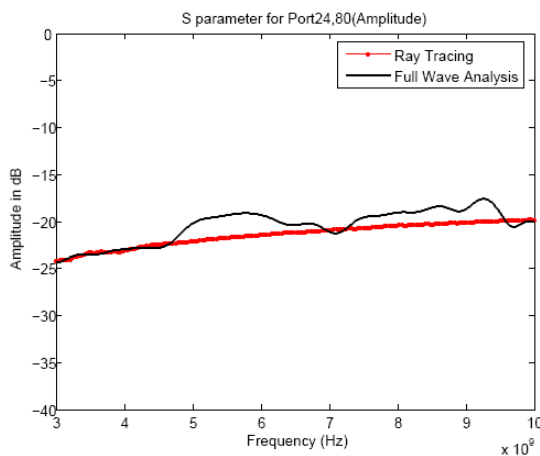


Figure 7. The amplitude coupling between port 24 and receiving port 80 across frequency band 3-10GHz.

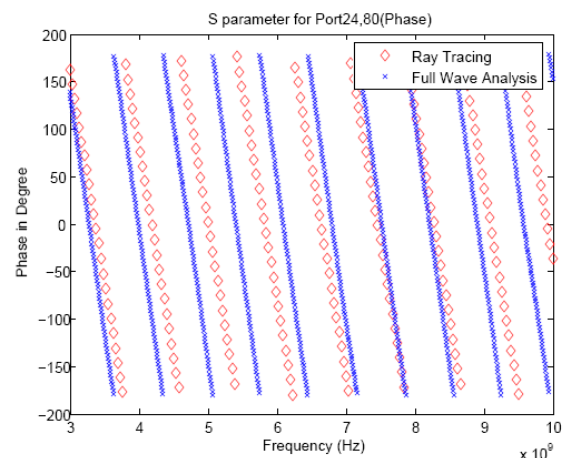


Figure 8. The phase coupling between port 24 and receiving port 80 across frequency band 3-10GHz.

## 5. References

1. W. Rotman and R. Turner, "Wide-angle microwave lens for line source applications," *IEEE Transactions on Antennas and Propagation*, vol. 11, 1963, pp. 623-632.
2. R. C. Hansen, "Design trades for Rotman lenses," *IEEE Transactions on Antennas & Propagation*, vol. 39, 1991, pp. 464-472.
3. C. Rappaport and A. Zaghoul, "Optimized three-dimensional lenses for wide-angle scanning," *IEEE Transactions on Antennas and Propagation*, vol. 33, 1985, pp. 1227-1236.
4. J. Dong, A. I. Zaghoul, and R. Rotman, "Non-Focal Minimum-Phase-Error Planar Rotman Lens," *USNC/URSI National Radio Science Meeting*, Boulder, Colorado, January 2008.
5. M. S. Smith, "Amplitude performance of Ruze and Rotman lenses," *Radio Electron*, vol. 53, pp. 329-336, 1983.
6. N. Yuan, J. S. Kot, and A. J. Parfitt, "Analysis of Rotman lenses using a hybrid least squares FEM/transfinite element method," *Microwaves, Antennas and Propagation, IEE Proceedings -*, vol. 148, 2001, pp. 193-198.
7. D. M. Pozer, "Microwave Engineering," *John Wiley & Sons*, 1998, pp. 288-292.
8. K. K. G. Avneesh Mittal, G.P. Srivastava, P.K. Singhal, R.D. Gupta, and P.C. Sharma, "Contour Integral Analysis of Planar Components," *Journal of Microwaves and Optoelectronics*, vol. 3, p. 15, 2003.
9. G. R. B. a. B. P. K. G. Razmafrouz, "Formulation of the Klopfenstein tapered line analysis from generalized nonuniform line theory," 1997.
10. O. Kilic and R. Dahlstrom, "Rotman lens beam formers for Army multifunction RF antenna applications," *IEEE Antennas and Propagation Society International Symposium*, vol. 2B, July 2005, pp. 43-46.
11. C. W. Penney, R. J. Luebbers, and E. Lenzing, "Broad band Rotman lens simulations in FDTD," *IEEE Antennas and Propagation Society International Symposium*, vol. 2B, pp. 51-54, July 2005.
12. R. H. Clarke, "Diffraction theory and antenna," *E. Horwood, Halsted Press*, 1980.
13. B. G. J.L. Cruz, E.A. Navarro, and V. Such, "The Phase Center Position of a Microstrip Horn Radiating in an Infinite Parallel-Plate Waveguide," *IEEE Transactions on Antennas and Propagation*, vol. 42, 1994, p. 4.
14. P. S. Simon, "Analysis and synthesis of Rotman Lenses," *22nd AIAA International Communications Satellite Systems Conference & Exhibit 2004*, May 2004.